Silencing of the Mitochondrial Ascorbate Synthesizing Enzyme L-Galactono-1,4-Lactone Dehydrogenase Affects Plant and Fruit Development in Tomato[1][W][OA]

Moftah Alhagdow, Fabien Mounet, Louise Gilbert, Adriano Nunes-Nesi, Virginie Garcia, Daniel Just, Johann Petit, Bertrand Beauvoit, Alisdair R. Fernie, Christophe Rothan, and Pierre Baldet*

Institut National de la Recherche Agronomique, Université Bordeaux 1, Université Victor Ségalen-Bordeaux 2, Institut Fédératif de Recherche 103, Unité Mixte de Recherche 619 sur la Biologie du Fruit, Centre de Recherche Institut National de la Recherche Agronomique de Bordeaux, BP 81, 33883 Villenave d'Ornon cedex, France (M.A., F.M., L.G., V.G., D.J., J.P., B.B., C.R., P.B.); and Max-Planck-Institut für Molekulare Pflanzenphysiologie, Am Mühlenberg 1, 14467 Potsdam-Golm, Germany (A.N.-N., A.R.F.)

L-Galactono-1,4-lactone dehydrogenase (EC 1.3.2.3) catalyzes the last step in the main pathway of vitamin C (L-ascorbic acid) biosynthesis in higher plants. In this study, we first characterized the spatial and temporal expression of *SlGalLDH* in several organs of tomato (*Solanum lycopersicum*) plants in parallel with the ascorbate content. P_{35S}:*Slgalldh^{RNAi}* silenced transgenic tomato lines were then generated using an RNAi strategy to evaluate the effect of any resulting modification of the ascorbate pool on plant and fruit development. In all P_{35S}:*Slgalldh^{RNAi}* plants with reduced *SlGalLDH* transcript and activity, plant growth rate was decreased. Plants displaying the most severe effects (dwarf plants with no fruit) were excluded from further analysis. The most affected lines studied exhibited up to an 80% reduction in *Sl*GalLDH activity and showed a strong reduction in leaf and fruit size, mainly as a consequence of reduced cell expansion. This was accompanied by significant changes in mitochondrial function and altered ascorbate redox state despite the fact that the total ascorbate content remained unchanged. By using a combination of transcriptomic and metabolomic approaches, we further demonstrated that several primary, like the tricarboxylic acid cycle, as well as secondary metabolic pathways related to stress response were modified in leaves and fruit of P_{35S}:*Slgalldh^{RNAi}* plants. When taken together, this work confirms the complexity of ascorbate regulation and its link with plant metabolism. Moreover, it strongly suggests that, in addition to ascorbate synthesis, GalLDH could play an important role in the regulation of cell growth-related processes in plants.

Vitamin C (L-ascorbic acid) has a huge importance for all living eukaryotic cells. In higher plants, ascorbate is the most abundant water-soluble antioxidant, acting to scavenge reactive oxygen species that are generated during photosynthesis, oxidative metabolism, and a wide range of stresses. In addition, ascorbate is involved in the regulation of several fundamental cellular processes such as photoprotection, the cell cycle, cell expansion, and in pathways of secondary metabolism such as the recycling of lipid-soluble α-tocopherol and ethylene biosynthesis. Although generally accepted, the mechanism by which ascorbate

participates in the cell developmental processes is not clearly established (for review, see Smirnoff, 2000). Much evidence supports the correlation between ascorbate content and its redox state and cell division and/or cell expansion (Horemans et al., 2003 and refs. therein).

Microorganisms, plants, and most animals produce ascorbate, however, a loss of the ability to synthesize ascorbate has occurred in primates and some other animals. Since the 1960s, the animal pathway has been completely characterized (Burns, 1960). It involves D-Glc as the initial precursor and the last step is catalyzed by a microsomal L-gulono-1,4-lactone oxidase, which oxidizes L-gulono-1,4-lactone to produce ascorbate. In plants, the ascorbate pathway is different from animals and has remained unsolved until recently, when convincing evidence in support of a novel pathway was established (Wheeler et al., 1998). To date, the pathway proposed by Wheeler et al. (1998) is the most commonly described in plants. Recently the last missing intermediate steps of the pathway have been elucidated (Laing et al., 2007; Linster et al., 2007). The last step in this pathway clearly involves the conversion of L-galactono-1,4-lactone (L-GalL) to ascorbic acid, a reaction catalyzed by the L-galactono-1,4-lactone dehydrogenase (here referred to as L-GalLDH),

an enzyme located in the inner membrane of the mitochondria (Bartoli et al., 2000). This reaction requires cytochrome *c* as a second substrate that is reduced as L-GalL is converted into ascorbate (Ôba et al., 1995).

In addition to this pathway, alternative ascorbate biosynthesis pathways have been proposed in plants. Agius et al. (2003) showed that during the ripening phase of strawberry (*Fragaria* spp.) fruit, ascorbate is produced via the reduction of D-GalUA to L-galactonic acid, which in turn is spontaneously converted to L-galactono-lactone, the immediate precursor of ascorbate. However, this pathway shares the requirement of L-GalLDH activity as the terminal step in ascorbate synthesis. In 2003, Wolucka and Van Montagu suggested an alternative pathway involving L-gulose as an intermediate for the de novo biosynthesis of vitamin C in plants. They showed that in vitro, GDP-D-Man-3,5-epimerase is capable of catalyzing two distinct epimerization reactions that produce either GDP-L-Gal or the novel intermediate, GDP-L-gulose. Nevertheless, the existence of all the enzyme machinery of this putative pathway has yet to be confirmed in vivo. Recently, Lorence et al. (2004) presented molecular and biochemical evidence proposing another possible biosynthetic route that utilizes myoinositol as a precursor. By overexpressing myoinositol oxygenase in Arabidopsis (*Arabidopsis thaliana*), they observed a 2- to 3-fold increase in ascorbate content in the leaf and discuss the possible contribution of myoinositol in ascorbate biosynthesis in plants. Following constitutive expression of the rat gene encoding L-gulono-lactone (L-GulL) oxidase, Jain and Nessler (2000) achieved a 4- and 7-fold increase of ascorbate content in lettuce (*Lactuca sativa*) and tobacco (*Nicotiana tabacum*) plants, respectively. L-GulL oxidizing activity has been reported in Arabidopsis by Davey et al. (1999) who measured L-GulL oxidizing activity and by Wolucka and Van Montagu (2003) who measured L-GulLDH-like activity.

Ascorbate is known to be a vital physiological metabolite in plants for major plant biochemical processes such as photosynthesis (Smirnoff, 1996; Noctor and Foyer, 1998), but also for controlling plant development as recently shown in root and other organs (Olmos et al., 2006). To investigate the physiological function of L-GalLDH in plants, we analyzed the effect of L-GalLDH silencing on ascorbate metabolism and its consequences for plant development. Since fruit is one of the major sources of ascorbate for the human diet, this study was carried out in tomato (*Solanum lycopersicum*), the model plant for fleshy fruit development. We report here that *SlGalLDH* silencing profoundly affects plant and fruit growth, probably through the alteration of the mitochondrial function and related changes in ascorbate redox state, particularly in the apoplast. Transcriptome and metabolome analyses of P_{35S}:*Slgalldh*^{RNAi} transgenic lines further suggest that phenotypic changes can be attributed to the resulting modifications in secondary and primary metabolism.

RESULTS

Ascorbate and L-GalLDH Distribution in Tomato Plant

To extend our understanding of the role of ascorbate in plant growth, we analyzed its distribution in a wide range of tomato organs, including vegetative tissues such as young and mature leaf, stem and root, and reproductive tissues such as flower and fruit at several stages of development (Fig. 1, A and B). In vegetative

Figure 1. *SlGalLDH* expression and ascorbate content in cherry tomato plants and fruit. A, Relative *SlGalLDH* transcript levels in young leaves (Yl), mature leaves (Ml), root (Rt), stem (St), flower (Fl) and in fruit at 10 DPA, 20 DPA, mature green (MG), orange (Or), and red ripe (RR) stages. Data obtained by semiquantitative RT-PCR were normalized against *Actin1* mRNA and are expressed as a ratio of arbitrary units. B, Total ascorbate content in the various tomato organs. Data represent mean ± SD of measurements of 10 organs per plant with six individual plants per line (*n* = 60). C, Detection of *SlGalLDH* transcripts in developing tomato organs by in situ hybridization. Longitudinal sections of shoot apical meristem (A), root apical meristem (B), young leaf (C), 9 mm flower bud (D), and cross section of fruit at 7 DPA (E) and 20 DPA (F) were prepared and analyzed as described in the experimental procedures. Hybridization signal appears as dark staining. Inserts are negative control corresponding to sense riboprobe. Scale bar = 500 μm.

organs, ascorbate content varied according to the tissue, with high levels in the leaf (young and mature) and comparatively low levels in the root. In flower and fruit, the ascorbate content remained very low (1.7–2.3 μmol per g fresh weight [FW]) compared to the leaf (6.8–7.9 μmol per g FW). The ascorbate concentration was constant throughout fruit development and comparable with the levels reported by Andrews et al. (2004).

Since L-GalLDH catalyzes the terminal step of the major pathway of ascorbate biosynthesis in plants (Wheeler et al., 1998), this enzyme is a good candidate for controlling the variations in ascorbate content in plants (Tamaoki et al., 2003; Bartoli et al., 2005; Tokunaga et al., 2005). Screening of tomato EST databases (SOL Genomics Network [SGN] and The Institute for Genomic Research tomato EST databases; http://www.sgn.cornell.edu and http://www.tigr.org/) allowed the identification of a single cDNA encoding L-GalLDH (named *SlGalLDH* for tomato L-*GalLDH*), which corresponds to a unique gene in tomato, as further confirmed by Southern-blot analysis (data not shown). Examination of *SlGalLDH* expression showed that *SlGalLDH* transcripts (Fig. 1A) and immunodetected *Sl*GalLDH protein (data not shown) were ubiquitously detected in the various tomato organs analyzed. The high *SlGalLDH* mRNA abundance in the leaf was in agreement with the high ascorbate content in this tissue (Fig. 1B), while other organs such as root or fruit did not display this relationship. Close examination of the spatial distribution of *SlGalLDH* transcripts in developing organs by mRNA in situ hybridization (Fig. 1C) further indicated that *SlGalLDH* transcripts were particularly abundant in tissues displaying a high cell proliferation activity such as the shoot apical meristem, the root apical meristem, young leaves, ovules, and stamen of flowers and young fruit at 10 DPA.

P_{35S}:*Slgalldh*^{RNAi} Transgenic Plants Do Not Display a Reduction of Ascorbate Content as Shown by the Capability to Maintain a Normal Ascorbate Synthesis

To further investigate the relationship between plant development and *SlGalLDH* activity in tomato, we generated transgenic plants expressing a *SlGalLDH*-specific RNA interference sequence fragment under the control of the cauliflower mosaic virus 35S promoter (hence named P_{35S}:*Slgalldh*^{RNAi} transformants). Among 12 independent primary P_{35S}:*Slgalldh*^{RNAi} transformants showing the presence of a single copy of the transgene, we selected four transgenic lines showing a range of phenotypic changes varying from severe (line 8) to moderate (line 5) and slight (lines 38 and 2) for further analyses on the next generation (T1 plants). To verify that the morphological changes observed in primary transformants were linked to the RNAi-mediated reduction in *SlGalLDH* mRNA, the detailed analysis of *SlGalLDH* mRNA and protein abundance and activity was performed in leaf and/or 20 and 42 DPA fruit from the corresponding T1 homozygous

P_{35S}:*Slgalldh*^{RNAi} transgenic lines 2, 5, 8, and 38 and from controls. In all transgenic lines, *SlGalLDH* mRNA, protein abundance, and residual *Sl*GalLDH activity were highly reduced by comparison with the control plants (Fig. 2), and no significant difference could distinguish the four transgenic lines on the basis of the expression/protein/activity data when statistical analysis was performed. Despite these strong effects, no remarkable variation could be observed in the total ascorbate content in young fully expanded leaves (6.75 ± 0.04 μmol per g FW) and 45 DPA red ripe fruits (1.82 ± 0.03 μmol per g FW) in the lines 2, 5, 8, and 38. The capacity of the transgenic plants to maintain the pool of total ascorbate constant was confirmed for the leaves of the lines 5 and 8 (Fig. 3). Leaves from the transgenic lines and controls accumulate ascorbate at similar rates when incubated with the ascorbate

Figure 2. *SlGalLDH* expression, protein, and activity in P_{35S}: *Slgalldh*^{RNAi} transgenic and control plants. A, *SlGalLDH* mRNA relative abundance was determined in young leaves (Yl) and fruit at 20 and 42 DPA (orange stage) in P_{35S}:*Slgalldh*^{RNAi} plants (line 2, 5, 8, and 38) and compared to control plants. Data obtained by semiquantitative RT-PCR were normalized against *Actin*1 mRNA and are expressed as percentage of control. Data represent mean ± SD of six individual plants per line. B, Immunodetection of *Sl*GalLDH protein in young leaves from P_{35S}:*Slgalldh*^{RNAi} line 2, 5, 8, and 38 and control plants. C, *Sl*GalLDH activity in young leaves from P_{35S}:*Slgalldh*^{RNAi} line 2, 5, 8, and 38 compared to control plants. Data represent mean ± SD of six individual plants per line. Asterisks above bars indicate values that were determined by the t test to be significantly different ($P < 0.05$) from control.
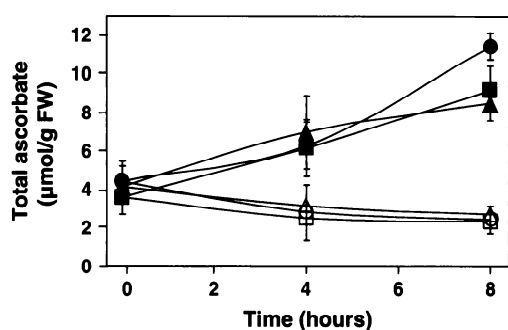
Figure 3. Ascorbate accumulation in tomato leaves. Leaf stripes from P_{35S}:*Slgalldh*^{RNAi} transgenic line 5 (△), line 8 (□), and control (○) plants were incubated in Murashige and Skoog (white symbols) or Murashige and Skoog containing 25 mm L-GalL (black symbols) in the light. Total ascorbate was assayed as described in "Materials and Methods." The error bars indicate SES ($n = 3$).

precursor L-GalL. Further investigations indicated that no viable plant with *Sl*GalLDH activity below the threshold level of 15% was ever recovered among the P_{35S}:*Slgalldh*^{RNAi} transformants, suggesting the essentiality of this activity.

P_{35S}:*Slgalldh*^{RNAi} Transgenic Lines Exhibit a Change in the Redox State of Ascorbate Associated with Alteration of the Mitochondrial Function in the Most Severely Affected Plants

Given the well established fact that ascorbate content of the leaf and ascorbate redox state depend on many environmental parameters, P_{35S}:*Slgalldh*^{RNAi} transgenic lines 5 and 8 and controls were grown in a phytotronic chamber to avoid any daily climate changes. Measurements of the total ascorbate content (reduced ascorbate [AsA] + dehydroascorbate) as well as of the AsA content were carried out during the development of these plants, from the seed up to the appearance of the first inflorescence (6 weeks after sowing), and within the developing fruit (Table I). Total ascorbate content in the seed and the young leaves of the apex was comparable in both transgenic and control plants. In the germinating seed of transgenic lines and the controls, approximately 90% of ascorbate was as the reduced form AsA. The leaf ratio of AsA to total ascorbate declined, both in the controls and the transgenic lines, throughout plant development (Table I). This effect, which was already noticeable in 21 d after sowing (DAS) transgenic plants, was not due to variations in total ascorbate content but to

Table I. *Ascorbate in tomato leaf and fruit of* P_{35S}:*Slgalldh*^{RNAi} *transgenic and control plants*

Reduced (AsA) and total ascorbate (Tot Asc) contents of P_{35S}:*Slgalldh*^{RNAi} line 8, line 5, and control plants were measured in young developing leaves from seedlings at the indicated DAS and in developing fruits at the indicated days postanthesis (DPA). Apoplastic ascorbate content was measured in the fully expanded fourth leaf of 6-week-old plants. The reduced/total ascorbate ratio was determined for all the samples. Data represent mean ± SD of six individual plants with two repeats per plant. The superscript a ([a]) indicates values that were determined by the t test to be significantly different ($P < 0.05$) from control.

Plant Stage (DAS)		$0_{(Seed)}$	15	21	28	42
Leaf				$\mu mol\ g^{-1}\ FW$		
AsA	Control	2.4 ± 0.2	1.5 ± 0.1	2.5 ± 0.3	2.6 ± 0.3	1.8 ± 0.1
	Line 8	2.5 ± 0.3	1.2 ± 0.1[a]	1.1 ± 0.1[a]	1.3 ± 0.1[a]	1.4 ± 0.2[a]
	Line 5	2.5 ± 0.2	1.1 ± 0.2[a]	1.2 ± 0.2[a]	1.4 ± 0.1[a]	1.3 ± 0.2[a]
Tot Asc	Control	2.5 ± 0.3	2.9 ± 0.2	4.5 ± 0.5	8.7 ± 0.7	8.5 ± 0.3
	Line 8	2.6 ± 0.2	2.9 ± 0.3	4.9 ± 0.5	6.1 ± 0.4	8.1 ± 0.3
	Line 5	2.6 ± 0.2	2.8 ± 0.3	5.5 ± 0.5	7.7 ± 0.1	8.1 ± 0.4
Ratio	Control	0.9	0.5	0.5	0.3	0.2
	Line 8	1	0.4	0.2	0.2	0.2
	Line 5	1	0.4	0.2	0.2	0.2
Fruit Stage (DPA)		10	20	30	38	42
Fruit						
AsA	Control	0.3 ± 0.1	0.4 ± 0.1	1.3 ± 0.1	1.7 ± 0.1	1.7 ± 0.2
	Line 8	0.5 ± 0.1[a]	0.9 ± 0.1[a]	1.6 ± 0.2[a]	1.6 ± 0.7	2.0 ± 0.2
	Line 5	0.6 ± 0.1[a]	0.7 ± 0.1[a]	1.6 ± 0.2[a]	1.8 ± 0.2	1.9 ± 0.2
Tot Asc	Control	1.6 ± 0.1	1.6 ± 0.1	1.6 ± 0.2	1.7 ± 0.1	2.0 ± 0.1
	Line 8	2.0 ± 0.1[a]	1.8 ± 0.3	1.7 ± 0.2	1.6 ± 0.7	2.2 ± 0.2
	Line 5	1.8 ± 0.1[a]	1.6 ± 0.1	1.6 ± 0.2	2.0 ± 0.2	2.1 ± 0.2
Ratio	Control	0.2	0.2	0.8	1	0.9
	Line 8	0.2	0.5	0.9	0.9	0.9
	Line 5	0.3	0.4	0.9	0.9	0.9
Leaf Apoplast		Control		Line 8		Line 5
				$nmol\ g^{-1}\ FW$		
AsA		85 ± 60		111 ± 10		121 ± 47
Tot Asc		648 ± 49		402 ± 47[a]		370 ± 104[a]
Ratio		0.1		0.3		0.3

variations in AsA content. The total ascorbate content of control fruit grown in a controlled environment chamber (Table I) was similar to that observed in control plants in the greenhouse (Fig. 1B). In the control fruit, 80% of total ascorbate was in the form of oxidized ascorbate during the cell division and expansion phases (10–20 DPA), while more than 90% of the total ascorbate was in the form of AsA in the ripening fruit. Total ascorbate content from transgenic lines 5 and 8 fruit were not significantly different from fruit of the control, except for the 10 DPA stage that exhibited a slightly higher ascorbate content. In contrast with the leaf, transgenic fruit from lines 5 and 8 exhibited a significant increase in AsA (Table I), mainly during the cell division and cell expansion stages of the fruit (10–30 DPA).

Because of the putative role of apoplastic ascorbate in the signaling processes modulating cell growth and development (Pignocchi and Foyer, 2003), we investigated the total and reduced ascorbate content in the apoplast of fully expanded leaves of 6-week-old P_{35S}:$Slgalldh^{RNAi}$ plants of transgenic lines 8 and 5. In the leaves of control plants, only 10% of the total ascorbate was found in the apoplast (648 ± 49 nmol per g FW) in agreement with previous findings of Noctor and Foyer (1998), and 10% to 15% of the apoplastic ascorbate was present as the reduced form. In the P_{35S}:$Slgalldh^{RNAi}$ transgenic line 8 and line 5, the reduced ascorbate pool remained very low (85–121 nmol per g FW), as in the controls. This occurred despite the

fact that the apoplastic total ascorbate content was decreased by about 50%, due to a reduction of the oxidized ascorbate pool (Table I).

Given that Millar et al. (2003) demonstrated that GalLDH activity is associated with the complex I of the mitochondrial electron transport chain and that it has been documented that respiration can control ascorbate synthesis in plants (Bartoli et al., 2006), intact leaf mitochondria were isolated to investigate respiratory parameters in the P_{35S}:$Slgalldh^{RNAi}$ transgenics. When tricarboxylic acid (TCA) cycle substrates pyruvate and malate were used to drive the electron chain, as well as when electrons entered the chain via succinate dehydrogenase by the addition of succinate, the respiration rate in the transgenic line 5 and 8 was identical to the controls (Table II). However, when external NADH dehydrogenases were engaged by addition of exogenous NADH, the respiration rate in P_{35S}:$Slgalldh^{RNAi}$ transgenic line 8 was increased by 1.6-fold whereas that in P_{35S}: $Slgalldh^{RNAi}$ transgenic line 5 was similar to the rate of control plant mitochondria. In the same order, a significant 2-fold activation of cyanide-insensitive (alternative oxidase) respiration that was inhibited by salicylhydroxamic acid (SHAM), was measured in mitochondria from P_{35S}:$Slgalldh^{RNAi}$ line 8. When no substrate, other than L-GalL, was used to introduce electrons flow to cytochrome c, the respiration rate in both transgenic lines was reduced to about 50% of that observed in mitochondria isolated from the control.

Table II. *Respiration and SlGalLDH activity in isolated mitochondria from leaves*

Respiration was measured in intact mitochondria prepared from young developing leaves of P_{35S}:$Slgalldh^{RNAi}$ line 8, line 5, and control plants as described in the "Materials and Methods." The reaction was conducted with 500 μg of mitochondria protein in 1 mL of respiration buffer in the presence of substrates at concentration as indicated. Prior to measuring the respiration in the presence of L-GalL, the mitochondria were incubated with 12.5 μM antimycine A. SlGalLDH activity was measured with 30 μg of mitochondrial protein as described in the "Materials and Methods." Data represent mean ± SD of seven or eight individual mitochondrial isolations. Superscript a ([a]) indicates values that were determined by the t test to be significantly different ($P < 0.01$) from control.

Respiration Electron Donor	Control	Line 5	Line 8
	nmol O_2 min^{-1} mg^{-1} protein		
2 mM NADH	48.7 ± 5.5	46 ± 4.5	73.6 ± 3.7[a]
+ 2.5 mM ADP	86.9 ± 8.4	75.8 ± 7.1	139.9 ± 4.1[a]
+ 2 mM KCN	10.4 ± 1.8	10.9 ± 3.8	20.6 ± 3.2[a]
+ 1 mM SHAM	8.4 ± 2.5	9.6 ± 1.9	12.5 ± 2.1[a]
Respiratory control	1.78	1.65	1.90
5 mM succinate	39.7 ± 7.8	48.4 ± 7.3	42.6 ± 10.9
+2.5 mM ADP	86.9 ± 13	97.1 ± 12.8	95.2 ± 20.7
Respiratory control	2.19	2.00	2.23
5 mM Pyr/malate	29.5 ± 4.5	34 ± 4.4	30.6 ± 3.4
+2.5 mM ADP	42.8 ± 8.3	47.6 ± 8.8	46.8 ± 4.6
Respiratory control	1.45	1.40	1.53
5 mM AsA	39.9 ± 6.4	42.1 ± 5.1	39.7 ± 3.9
2.5 mM TMPD	409.5 ± 32.5	393.7 ± 44.3	380.1 ± 45.4
4.2 mM L-GalL	9.7 ± 0.9	5 ± 0.9[a]	5.4 ± 0.6[a]
+10 μM cytochrome c	13.4 ± 1.6	6.9 ± 0.7[a]	6.5 ± 0.8[a]
SlGalLDH Activity	Control	Line 5	Line 8
	nmol cytochrome c min^{-1} mg^{-1} protein		
	96 ± 15.1	49.6 ± 10.5[a]	20 ± 5[a]

The difference in the respiratory activities in the different transgenic lines demonstrates that a threshold level of 50% must be exceeded for the reduction of GalLDH abundance to impact the mitochondrial electron transport chain.

Transgenic Plants with Reduced L-GalLDH Activity Display a Reduced Plant Growth Rate and Fruit Size

When T1 transgenic plants were grown in the greenhouse, it soon became apparent that the growth of the aerial parts was reduced compared with that of the controls. Detailed characterization of this effect revealed that the germination rate, the plant growth rate, the fruit weight, and the diameter were all reduced (Fig. 4). When this experiment was replicated in a growth chamber with tightly controlled growth conditions similar results were obtained. To investigate how the reduction in *Sl*GalLDH mRNA abundance, protein, and activity could affect plant growth and morphology in the transgenic plants, we conducted more detailed analyses of lines 2, 5, 8, and 38. Given the reduction in aerial yield in the P_{35S}:*Slgalldh*^{RNAi} transformants and the importance of ascorbate for the photosynthetic process, we next assessed to what extent the transgenic plants exhibited altered photosynthetic rates. The rate of CO_2 assimilation was measured on fully expanded leaves of the transformant and control plants at incident irradiance of between 200 to 1,000 μmol m^{-2} s^{-1}. At this light intensity range, the CO_2 assimilation curve was linear and the calculated photosynthetic rate, 16.2 $\pm$ 0.8 nmol CO_2 per μmol photon, was invariant in transformants with respect to the controls. It is noteworthy that chlorophyll content was also unaltered (1.4 $\pm$ 0.2 mg chl per g FW).

In contrast, leaf size was strongly affected in the P_{35S}:*Slgalldh*^{RNAi} transgenics, which resulted from a 25% reduction in leaflet area in the most strongly inhibited lines (Fig. 5, A and B). Analysis of epidermal cell size indicated that this result does not stem from a reduction in cell number but rather from a reduction in cell size, which was also reduced by about 25% compared to that of the control (Fig. 5B). Similar observations were made in fruit, which exhibited a cell size reduction of 15% to 22% in the transgenic lines 8 and 5, despite exhibiting an unaltered ripening period (45 d). The analysis of a cross section taken from the equatorial area of a red ripe fruit revealed that the transgenic lines produced fruits with a thinner pericarp. Given that it is very difficult to obtain suitable samples from red ripe fruit for histological analysis (Cheniclet et al., personal communication), we compared the thickness of the pericarp in fruits at 20 DPA, at which stage the fruits reached 85% of their final size. Cytological analysis revealed that the fruit pericarp thickness was significantly decreased in all lines (Fig. 5C). Detailed comparisons indicated that this was a result of a cell size reduction in the pericarp rather than an alteration in the number of cell layers (Fig. 5D).

Figure 4. Phenotypic comparison between P_{35S}:*Slgalldh*^{RNAi} transgenic and control plants. A, Germination and plant growth. Left and middle section, seedlings from P_{35S}:*Slgalldh*^{RNAi} line 2, 5, 8, and 38 and from control at 10 DAS; right section, 6-week-old plants from severely affected P_{35S}:*Slgalldh*^{RNAi} line 5 and from control. B, Growth kinetic. Plant height from P_{35S}:*Slgalldh*^{RNAi} lines 5 and 8 and from control were measured every 4 d starting from 6 d after germination. Data represent mean $\pm$ SD of 10 individual plants. C, Fruit size. Top section, pictures of ripe fruit from P_{35S}:*Slgalldh*^{RNAi} lines 2, 5, 8, and 38 and from control; bottom section, fruit diameter measured on 42 DPA fruit. Data represent mean $\pm$ SD of 10 fruits per plant with six individual plants per line ($n = 60$ fruits). Asterisks above bars indicate values that were determined by the t test to be significantly different ($P < 0.05$) from control.

Functional Classification of Genes Expressed in Leaf and Ripening Fruit of P_{35S}:*Slgalldh*^{RNAi} Transgenic Lines

To investigate the possible contribution of changes in transcript expression triggered by the reduction in

(*P* value < 0.02, four independent slide hybridizations, including two dye swaps and two replicates per slide) in line 8 versus control plants (see http://cbi.labri.fr/outils/data/Tomato/VitC/sup.html). A previously reported and recently further enhanced annotation of the genes represented on the TOM1 array combined with the MapMan ontology (Thimm et al., 2004; Urbanczyk-Wochniak et al., 2006) was used for analyses (see http://cbi.labri.fr/outils/data/Tomato/VitC/sup.html). More detailed analyses were performed on the most differentially expressed genes selected using a mean ratio threshold >1.6, representing 35 genes in the fruit and 83 genes in the leaf; of these, seven genes in the fruit and 19 in the leaf encoded proteins with unknown functions or, alternatively, presented no homology with known genes (Table III). Most of the genes identified were up-regulated in the leaf from the transgenic lines, only 5% of the differentially expressed genes were repressed in either leaf or fruit.

Classification of the known genes into the different functional categories defined by the Munich Information Center for Protein Sequences (http://mips.gsf.de/projects/funcat) indicated the following distribution in leaf and fruit tissues: In the leaf, a first group (I) contained 18 stress-related transcripts known to be induced by various stresses (wounding, cold, light, etc.), such as geranylgeranyl reductase (Giannino et al., 2004) and Glu decarboxylase (Bouché and Fromm, 2004). A second group (II) contained 21 sugar metabolism-related genes involved in photosynthesis, carbohydrate, and cell wall metabolism, e.g. the Rubisco activase, the xyloglucan endotransglucosylase hydrolase, the PSII (or PSI) proteins, and the glyceraldehyde-3-P dehydrogenase. A third group (III) of 10 transcripts included several genes possibly involved in regulatory processes, for example a protein phosphatase 2C (PP2C) phosphatase, a MADS-box protein TDR3, and an F-box protein. A last group (IV) contained 10 genes encoding miscellaneous proteins related to transport and various metabolisms.

In the fruit, group I contained six stress-related transcripts including three heat shock proteins. Group II contained six transcripts, two of them encoding a PSII protein and Rubisco. Group III contained 12 transcripts, including a Ser/Thr protein kinase, a PP2C phosphatase, a WRKY type, and the agamous TAG1 transcription factors and a GA 20-oxidase. Remarkably, the *MULTIPROTEIN BRIDGING FACTOR1* (*MBF1*) gene, a transcriptional coactivator known to induce the expression of stress-related genes involved in plant defense (Suzuki et al., 2005) and expressed in tomato (Zegzouti et al., 1999), displayed a high expression in the transgenic line 8 (ratio >4.5) compared to control plants. In addition, several genes involved in ethylene signal transduction such as the ethylene receptor ETR2 or in ethylene response, including the MBF1 factor, the ethylene-responsive protein ERF1, and the ripening-regulated protein DDTFR8 (Zegzouti et al., 1999) were strongly induced in the ripening fruit. Group IV contained four genes encoding proteins related to miscellaneous metabolisms.

Figure 5. Microscopic analysis of leaf and fruit pericarp of P_{35S}:*SlgalldhRNAi* transgenic and control plants. A, Micrograph of collodion imprint of adaxial epidermal cells of fully expanded fourth leaf from P_{35S}:*SlgalldhRNAi* line 8 and control plant. Scale bar = 100 μm. B, Leaflet area and adaxial epidermal cell size of fully expanded fourth and fifth leaf from P_{35S}:*SlgalldhRNAi* lines 5 and 8 and control plant. The region examined was located between two midveins in the first 5 cm of the leaflet. Data represent mean ± SD of four individual leaves per plant with six plants per line (*n* = 24). C, Micrograph of pericarp section of 20 DPA fruit from P_{35S}:*SlgalldhRNAi* line 5, 8, and control. Scale bar = 200 μm. D, Pericarp thickness, number of cell layers, and cell size of 20 DPA fruit from P_{35S}:*SlgalldhRNAi* lines 2, 5, 8, and 38 and control. Measurements were done by in situ observations of a region of interest located between the vessels in transverse pericarp sections from the equatorial region of the fruit. Data represent the mean ± SD of pericarp sections from 10 fruits per plant with six individual plants per line (*n* = 60). a, Values that were determined by the *t* test to be significantly different (*P* < 0.05) from control.

*Sl*GalLDH activity and/or variations in ascorbate redox state to the morphological and cellular alterations of transgenic plants (Figs. 4 and 5), we compared the transcript expression profiles of a fully expanded fourth leaf and of 42 DPA (orange) fruit in the severely affected line 8 and in control plants. Among the 13,400 cDNAs corresponding to 8,700 transcripts present on the TOM1 tomato microarray analyzed, 1,269 in the leaf and 92 in the fruit were significantly different

Table III. *Genes differentially expressed in leaf and orange fruit of P_{35S}:Slgalldh^{RNAi} line 8 versus control plants*

SGN[a]	Description	P Value[b]	Ratio[c]
Leaf			
Group I: Stress			
U212549	Glu decarboxylase	0.008	2.4
U212565	Ripening-associated membrane protein	0.013	1.7
U212578	Alcoholacyltransferase	0.009	−1.6
U212870	Polyphenol oxidase chloroplastic	0.010	1.6
U212989	TSI-1 protein	0.016	1.7
U213021	Wound-induced proteinase inhibitor	0.013	1.6
U212874	Wound-induced proteinase inhibitor	0.008	2.3
U212973	Metallothionein-like protein	0.017	1.6
U213190	Cold-induced glucosyltransferase	0.015	1.7
U213588	Protease inhibitor	0.010	2.1
U213613	Ethylene-responsive proteinase inhibitor	0.012	1.9
U214777	Pro-rich protein	0.010	2.3
U216788	Pro synthetase associated protein	0.008	2.5
U215124	Ultraviolet-B repressible protein	0.014	1.6
U224685	Glucan-1,3-β-glucosidase	0.010	2.1
U226439	UDP-glucuronosyl transferase	0.013	1.7
U218272	Ser protease	0.017	1.8
U214067	Geranylgeranyl reductase	0.008	1.8
Group II: Photosynthesis; Carbon and Cell Wall Metabolism			
U212564	Plastidic aldolase	0.011	1.7
U212700	Plastidic aldolase	0.011	1.8
U212863	Chlorophyll *a/b*-binding protein precursor	0.011	1.6
U212865	Chlorophyll *a/b*-binding protein precursor	0.008	2.3
U212939	Rubisco activase	0.009	1.9
U212940	Rubisco activase	0.014	1.8
U212941	Rubisco activase	0.010	2.3
U213031	Plastocyanin chloroplast precursor	0.014	1.9
U213044	Xyloglucane endotransglucosylase	0.009	1.9
U213080	Carbonic anhydrase precursor	0.012	1.7
U213214	PSII core complex proteins	0.011	1.8
U213287	PSII core complex proteins	0.010	1.9
U213381	PSI reaction center subunit	0.012	1.9
U213390	PSI reaction center subunit	0.011	1.7
U213493	Pectine esterase	0.008	1.7
U213559	Pectine esterase	0.010	1.7
U214487	Extensin	0.011	1.6
U216405	Xyloglucane endotransglycosylase	0.014	1.7
U216855	Thioredoxin	0.008	−1.6
U220664	Glycerol-3-P acyltransferase	0.008	1.9
U225515	Glyceraldehyde-3-P dehydrogenase	0.011	1.8
Group III: Signal Transduction and Hormones			
U212854	Calmodulin	0.009	1.6
U214384	Apetala2-like protein	0.015	1.6
U214458	RNA-binding protein	0.011	1.7
U220213	MADS-box protein TDR3	0.011	1.9
U221524	Ser/Thr protein kinase	0.010	2.0
U222333	Ethylene response binding protein	0.011	1.6
U223492	F-box protein	0.017	−2.1
U225548	PP2C	0.011	1.7
U213123	Arg decarboxylase	0.011	1.6
U215755	Auxin-binding protein	0.012	2.3
Group IV: Miscellaneous			
U213050	Glycolate oxidase	0.010	1.8
U213604	Inorganic pyrophosphatase	0.014	1.7
U213912	Aminomethyltransferase	0.010	1.8
U214617	Acetyl-CoA C-acyltransferase	0.013	1.9

(Table continues on following page.)

Table III. *(Continued from previous page.)*

SGN[a]	Description	*P* Value[b]	Ratio[c]
U215017	Sterol C-methyl transferase	0.010	1.7
U216066	Vacuolar ATP-synthase subunit	0.010	1.8
U216256	Cytochrome *c* oxidase	0.012	1.6
U216323	Translation initiation factor	0.011	1.6
U216736	Ca2+-ATPase	0.015	1.6
U216923	Lipid transfer protein	0.010	1.7
U217914	Metal-transporting P-type ATPase	0.012	1.8
U217993	Adaptin	0.012	1.6
U218299	Ribosomal protein	0.011	1.6
U218653	Sterol C-methyl transferase	0.011	1.6
U240467	Developmental protein related	0.008	1.8
Orange Fruit			
Group I: Stress			
U212932	Heat shock protein	0.012	2.1
U213790	Acidic endochitinase	0.011	1.9
U216459	Gly-rich protein	0.012	2.0
U216468	Cytosolic heat shock protein	0.011	4.2
U218323	Heat shock protein	0.011	2.6
U214174	Coumarate-CoA ligase	0.012	2.2
Group II: Photosynthesis; Carbon and Cell Wall Metabolism			
U213287	PSII	0.013	2.9
U213624	Pyruvate decarboxylase	0.012	2.3
U216001	Extensin class I	0.016	1.6
U216086	Carbohydrate kinase	0.014	2.5
U225512	Rubisco	0.011	2.1
U225539	Glc-1-P adenylyl transferase	0.016	1.7
Group III: Signal Transduction and Hormones			
U213126	Calreticulin	0.018	1.6
U214610	WRKY protein	0.012	−1.6
U215004	AGAMOUS protein	0.011	1.6
U216554	Hydroxysteroid dehydrogenase	0.018	2.3
U216991	Ser/Thr protein kinase	0.011	2.0
U217359	MBF1	0.013	4.5
U219135	Ethylene responsive factor JERF2	0.018	1.6
U219631	GA 20-oxidase	0.017	1.9
U229641	Ethylene-receptor 2 ETR2	0.016	1.6
U221533	PP2C	0.011	1.8
U223066	AP2/ERF-type protein	0.018	−1.8
U225322	Ser/Thr protein kinase	0.016	1.7
Group IV: Miscellaneous			
U213332	Peptidyl prolyl isomerase	0.017	2.0
U216689	Threonyl-tRNA synthetase	0.019	1.8
U217998	Metal transporter	0.011	1.8
U219908	Ripening regulated protein DDTFR8	0.013	4.5

[a]SGN tomato unigenes identification number of cDNA spotted on TOM1 microarray (http://www.sgn.cornell.edu/search/direct_search.pl?search=unigene). [b]Probability of the *t* test. [c]Mean ratio of the normalized data between P_{35S}:*Slgalldh*^{RNAi} line 8 and control plants.

Changes in Metabolite Profiles in the P_{35S}:*Slgalldh*^{RNAi} Transgenic Lines

We next analyzed the relationship between the phenotypes of three P_{35S}:*Slgalldh*^{RNAi} lines (2, 8, and 38) and the changes in the redox state of ascorbate via a metabolomic approach. We analyzed the major pathways of primary plant metabolism by using an established gas chromatography-mass spectroscopy method (Fernie et al., 2004). As would be expected, the metab-

olomic analyses confirmed the rank order of the lines, 5 and 8 being the most affected at the metabolic level (Supplemental Table S2). Furthermore, expanding leaves and orange fruits behaved inversely at the metabolic level (Fig. 6; Supplemental Table S2). In leaves, metabolite analyses revealed a decrease in the levels of the major amino acids whereas some of them, Cys, Pro, Thr, and Val increased. In contrast, in orange fruit, the levels of amino acids were largely unaffected, with the

Figure 6. Description of central metabolism of fully expanded leaves and orange fruits from plants of the P_{35S}:$Slgalldh^{RNAi}$ line 8. Metabolite content of leaf and orange fruit were determined as described in "Materials and Methods." Data were normalized with respect to the mean response calculated for the control (to allow statistical assessment, individual samples from this set of plants were normalized in the same way). A color code indicates that values for metabolite content were determined by the t test to be significantly different ($P < 0.05$) from control (empty vector transgenic plant). Metabolites marked in red indicate that their relative content was decreased with respect to the control, and those marked in blue were increased. Examples of metabolite changes are represented by the values (mean ± SE) of determinations of six individuals plants with 10 leaves and fruits of each plant. Abbreviations: G6P, Glc-6-P; 3-PGA, 3-phosphoglycerate; F6P, Fru-6-P; FA16:0, palmitate; FA18:0, stearate; PEP, phosphoenolpyruvate.

exception of Val and Met that increased and of Pro that was reduced by half, significantly in the case of line 8 (Fig. 6). In leaves, the level of TCA cycle intermediates was significantly reduced, with the exception of succinate that displayed a slight but significant increase (Fig. 6). Among other organic acids, threonic acid, which corresponds to a degradation product of the ascorbate turnover pathway, displayed an increase in all transformants, whereas the opposite was observed for the γ-aminobutyric acid (GABA) content. In orange fruits, the content of the TCA cycle intermediates was unchanged; however, the succinate content displayed an increase similar to that observed in the leaf. The most important change was for malate, which increased by up to 4.6-fold in line 8. Among the other organic acids, GABA accumulated up to 2.8-fold in fruit of line 8 whereas threonate was slightly reduced. Analysis of the leaf carbohydrate content revealed that the P_{35S}:$Slgalldh^{RNAi}$ transgenic lines were characterized by increases in Fru and Suc, as well as other sugars linked to the cell wall metabolism like Ara, Gal, Man, Rha, and raffinose, which increased by up to 5-fold in line 8. Myoinositol increased significantly in both SlGalLDH lines. In fruit, the level of sugars was

largely unaffected; however, the levels of some cell wall-related sugars and myoinositol were significantly reduced, whereas sorbitol and mannitol increased. Interestingly, GalUA, an intermediate of the alternative ascorbate biosynthesis pathway and a degradation product of the cell wall pectins during fruit ripening (Agius et al., 2003) decreased significantly in all transgenic plants. Among the other compounds analyzed, it is interesting to note that intermediates involved in membrane biogenesis like C16:0 and C18:0 fatty acids were increased (Supplemental Table S2).

DISCUSSION

The RNAi-reduced expression of SlGalLDH in tomato leads to plants with a residual L-GalLDH activity showing several defects in growth rate and organ size (Figs. 4 and 5). All these observations are consistent with the preferential localization of SlGalLDH transcripts in tissues actively engaged in cell division and/or expansion such as root tips or floral meristem and young fruit, as well as the photosynthetic leaves (Fig. 1). Among the primary transformants, two P_{35S}:$Slgalldh^{RNAi}$ transgenic lines showed the most extreme reduction in

total ascorbate content (85–170 nmol ascorbate per g FW) and displayed very severe growth defects such as stunted plants with deformed leaves. These plants remained unable to set flowers and fruits and could not be propagated by cuttings, which prevented their use in subsequent studies. This result suggests the existence of a threshold level of L-GalLDH activity, below which ascorbate content and consequently plant growth are so severely impaired that reduction in L-GalLDH activity can be lethal to the plant. Another intriguing result to emphasize is the apparent complexity of ascorbate regulation in different plant tissues. Silencing of GalLDH had opposite effects in leaves and fruits on metabolic profiles and ascorbate redox state (Supplemental Tables S1 and S2). This discrepancy may result from the different functions of these organs, source (leaves), or sink (fruit). Most probably, it may result from the close relationship between photosynthetic electron transport in chloroplasts and ascorbate pool size in leaves, suggested by Yabuta et al. (2007). Silencing GalLDH has a significant effect on both the transcriptome and metabolome, thus giving emphasis to the importance of the role of GalLDH in plants, and data presented here allow us to draw the following conclusions.

SlGalLDH Activity Is Essential for Plant and Fruit Growth in Tomato

How the plant compensates for SlGalLDH reduction in the P_{35S}:Slgalldh^{RNAi} transgenic lines studied (Table I; Fig. 2), to maintain a pool of ascorbate similar to the controls, remains an open question. The most plausible explanation is that residual SlGalLDH activity is high enough in the transgenic lines we tested to sustain sufficient ascorbate biosynthesis. This is supported by the experiment of incubation with L-GalL (Fig. 3) showing that even in lines 5 and 8, in which the activity was severely affected, the ascorbate accumulation rate was maintained at the same level as that of control plants. However, we cannot rule out that the maintenance of the ascorbate pool is associated with a reduction of its turnover. The metabolic analysis of fruit from P_{35S}:Slgalldh^{RNAi} lines gives some support to this hypothesis in that a significant decline in the content of threonate (Fig. 5), the end product of one of the known pathways of ascorbate degradation (Green and Fry, 2005; DeBolt et al., 2006), exists. However, it should be noted that in leaves from the transgenic plants, threonate and its precursor dehydroascorbate strongly accumulated (Fig. 6; Supplemental Table S2), raising the possibility of different regulation of ascorbate degradation in vegetative and reproductive organs. Another possible way for these plants to maintain the vital pool of ascorbate is the activation of alternative pathways of ascorbate biosynthesis (Agius et al., 2003; Wolucka and Van Montagu, 2003; Lorence et al., 2004). The pathway described by Agius et al. (2003) also requires L-GalLDH to catalyze ascorbate biosynthesis. While the

gulose pathway proposed by Wolucka and Van Montagu (2003) still remains hypothetical, another plant pathway involving myoinositol has been proposed by Lorence et al. (2004). Elevated myoinositol levels are usually associated with stress conditions (Nelson et al., 1998). In P_{35S}:Slgalldh^{RNAi} lines, the significant increase in myoinositol level in the leaf (Fig. 6; Supplemental Table S2) could, thus, be indicative of the function of this alternative pathway in vegetative organs.

Reduced SlGalLDH Expression May Affect Cell Growth by Modifying Mitochondrial-Related Energy Metabolism

Given the accepted role of ascorbate in photosynthesis, the hypothesis of an alteration in the photosynthetic capacity could have been anticipated in the P_{35S}:Slgalldh^{RNAi} lines. However, our results clearly indicate that the reduced organ growth in the P_{35S}:Slgalldh^{RNAi} lines does not result from an impaired photosynthesis, which was not affected in these plants despite the fact that more than 10 of the significantly up-regulated transcripts were directly related to photosynthesis (Table III).

One of the most important metabolic consequences that could explain cell growth impairment in the leaf is the change of mitochondrial function, as shown by the alteration of the Kreb's cycle (Fig. 6) and respiration rate observed in the most affected line 8 (Table II). This finding is interesting regarding the results of a recent study that supports a strong functional link between respiration and ascorbate synthesis and suggests that L-GalLDH is associated with complex I of the mitochondrial electron transport chain (Millar et al., 2003). This functional association may explain why the capacity of L-GalLDH is variable dependent on growth light intensity (Smirnoff, 2000; Bartoli et al., 2006) since the activity of the mitochondrial electron transport chain also varies with light intensity (Raghavendra and Padmasree, 2003). It is thus conceivable that the removal of most of the L-GalLDH protein from complex I affects electron transport. In support of this theory, levels of organic acids of the TCA cycle are decreased in leaf and fruit and some changes in metabolite and transcript profiles are similar to those observed in illuminated leaves of tomato deficient in TCA cycle enzyme expression (Carrari et al., 2003; Urbanczyk-Wochniak et al., 2006). Furthermore, the results presented here are comparable to those observed in the CMSII mutant of tobacco, which is deficient in complex I function, has a severely inhibited growth phenotype, and displayed constitutively high alternative oxidase activity associated in particular with high alternative NAD(P)H dehydrogenase activity (Dutilleul et al., 2003). However, some divergences exist since the CMSII mutant was able to permanently adjust the cell redox homeostasis, which was not the case in the P_{35S}:Slgalldh^{RNAi} lines, at least in the case of ascorbate. Interestingly, our results corroborate the

work of Millar et al. (2003) who showed that respiration controls ascorbate synthesis in plants, particularly through a link between complex I and GalLDH protein. In the transgenic tomato plants described here, the reduction in *Sl*GalLDH activity appears to directly affect the efficiency of the alternative respiratory pathway and consequently the mitochondrial function, with the combination of changes in ascorbate and respiration resulting in a consequent alteration of the cell growth processes. Since several enzymes of the Kreb's cycle are redox regulated (Balmer et al., 2004), it is conceivable that any variation in the redox state of the plant may have additional effects on plant growth by modulating energy pathways.

Growth of P_{35S}:*Slgalldh*^{RNAi} Plants Is Adjusted through Changes in Transcript Expression and Metabolic Profiles

Very little is known about the exact mechanisms by which ascorbate regulates cell growth in plants (Smirnoff, 1996; Noctor and Foyer, 1998). This is all the more complex since in P_{35S}:*Slgalldh*^{RNAi} plants the vegetative and reproductive tissues behaved oppositely with regard to the ascorbate redox state in comparison to the controls (Table I). Organ growth in plants depends on the processes of cell division and cell expansion that are separately controlled during development (Mizukami, 2001). In the P_{35S}:*Slgalldh*^{RNAi} transgenic plants, the cell division phase was not affected, since in the most severely affected line 8, the reduction in leaflet and fruit size was clearly related to changes in cell size and not in cell number (Fig. 5). Our results are in contrast with the work carried out in BY-2 cells by Tabata et al. (2001) showing that *GalLDH* antisense transgenic cell lines displayed a 30% reduction of ascorbate content compared to the wild type, and significant changes of division and growth processes. This discrepancy can be attributed to the fact that BY-2 cells are undifferentiated plant material, in contrast to whole plants organs (Geelen and Inzé, 2001). A putative mechanism by which ascorbate could influence cell enlargement has been proposed by Smirnoff (2000). This hypothesis is based on the existence of an ascorbate redox cycle that could stimulate cell expansion through the extrusion of protons in the cell wall, in agreement with the acid growth theory (Rayle and Cleland, 1992). Accordingly, it is tempting to suggest that the reduction in *Sl*GalLDH activity in P_{35S}:*Slgalldh*^{RNAi} transgenic plants has led to the reduction in plant cell size and this causes a change in apoplastic ascorbate (Table I). Recent genetic evidence from tobacco plants expressing sense and antisense ascorbate oxidase indicates that alteration of ascorbate oxidase activity and ascorbate redox state of the apoplast may to some extent affect plant growth (Pignocchi et al., 2006).

Several recent reports have suggested that plant mitochondria are part of signaling pathways known as the mitochondrial retrograde regulation (MRR), and

participate in the response to oxidative stress (for review, see Rhoads and Subbaiah, 2007). According to the MRR process, changes in the mitochondrial function trigger altered nuclear transcript expression. Much of what is known about plant MRR turns around the response to a dysfunctional mitochondrial electron transport chain and induction of genes encoding enzymes involved in the recovery of mitochondrial function, such as AOX and alternative NAD(P)H dehydrogenases as well as genes encoding proteins involved in the maintenance of the redox homeostasis, such as gluthathion reductase, catalases, ascorbate peroxidases, and superoxide dismutases. Variations in ascobate redox state could in turn modulate the cross-talk between several defense and growth regulating pathways to adapt the plant to its challenging environment. Overall our data are consistent with the hypothesis, suggesting that the changes in ascorbate redox state in the plant induced by the silencing of *SlGalLDH* mimic stress-related MRR signaling pathways, inducing a set of stress- and defense-related genes. Hence, the transcriptome analysis revealed that a high proportion of the genes differentially expressed in the leaf and fruit from P_{35S}:*Slgalldh*^{RNAi} lines are known to be induced by a wide range of biotic or abiotic stresses. Most of them are hormone-responsive genes with functions in signaling for plant-defense and stress-response pathways (Table III). This is particularly obvious in the fruit from P_{35S}:*Slgalldh*^{RNAi} plants where the transcriptional coactivator MBF1, previously shown to be ethylene regulated in tomato (Alba et al., 2004), is highly expressed (>4.5-fold change). Constitutive expression of *MBF1* gene in Arabidopsis confers to the plants an enhanced tolerance to environmental stresses and to bacterial infection, possibly by modulating the ethylene-response signal transduction pathway (Suzuki et al., 2005). Besides, a wide range of genes up- or down-regulated in the transgenic plants are also involved in signal transduction pathways and may participate in the regulation of developmental processes (e.g. the MADS-box gene *Agamous*; Ferrario et al., 2006). The tight connection between ascorbate content and/or apolastic ascorbate redox state and hormonal signaling for plant defense was recently pinpointed in studies on the Arabidopsis ascorbate mutant *vtc1*, which is affected in abscisic acid synthesis and response (Pastori et al., 2003) and on the ascorbate oxidase overexpressing tobacco lines showing altered sensitivity to auxin (Pignocchi et al., 2006). Similarly, the metabolic analysis revealed significant changes for several stress-related compounds, e.g. Pro (Parre et al., 2007) and GABA (Lancien and Roberts, 2006). Taken all together, the extensive analysis of P_{35S}:*Slgalldh*^{RNAi} plants further highlights the complexity of ascorbate regulation and its relation with different aspects of plant metabolism and also plant tissues, e.g. the photosynthetic leaf and the developing fruit, since they display both distinct (metabolism) and common (signaling) features with respect to ascorbate.

MATERIALS AND METHODS

Plant Material and Growth Conditions

Cherry tomato (*Solanum lycopersicum* 'West Virginia 106') plants were grown in a greenhouse with supplemental lighting when needed with a light period of 14/10 h, under a thermoperiod of 25°C/20°C, and watered daily three times with a solution at pH 5.8 containing oligoelements plus 3.5 mM KNO_3, 1 mM K_2SO_4, 2 mM KH_2PO_4, 6 mM $Ca(NO_3)_2$, and 2 mM $MgSO_4$, until the stage fruit set of the first truss, and then 4 mM KNO_3, 1.5 mM K_2SO_4, 1.5 mM KH_2PO_4, 4 mM $Ca(NO_3)_2$, and 1.5 mM $MgSO_4$. For in vitro culture, plants were grown on one-fourth Murashige and Skoog basal Murashige and Skoog medium (Kalys-Duchefa) containing 3% Suc under 14/10 h photoperiod at 400 μmol m^{-2} s^{-1} and at 25°C. Tomato fruits were harvested at various developmental stages according to the number of DPA and fruit diameter. Prior to all biochemical and molecular analysis, samples were quickly frozen in liquid nitrogen, ground to fine powders, and stored at −80°C until use.

Determination of Photosynthetic Activity

Photosynthetic activity of attached leaves was measured with a CO_2 analyzer using infrared detection (LCA3; Analytical Development Corporation).

Respiration Determinations of Isolated Mitochondria

To measure mitochondrial respiratory parameters, mitochondria were prepared from young leaf (50–100 g) following the method of Holtzapffel et al. (2002). After isolation and purifications steps, the mitochondria were washed and resuspended in the incubation medium containing 10 mM TES, pH 7.2, 300 mM Suc, 0.1% (w/v) bovine serum albumin (BSA), 5 mM Kh_2PO_4, 5 mM $MgCl_2$, and 10 mM KCl to a concentration of 10 to 50 mg protein mL^{-1}. Respiration measurement was performed using O_2 electrode (782 Oxygen meter, Strathkelvin Instruments) in the presence of several electron donors and respiratory inhibitors like KCN and SHAM. Mitochondrial integrity was determined according to Holtzapffel et al. (2002) and was generally between 75% to 85%.

Cytological Analyses

Pericarp cell number and size were measured in fruits as described by Cheniclet et al. (2005). The cell size of leaflet epidermis was measured by applying a thin layer of collodion 4% resin (Merck) of about 2 to 3 cm^2 on the adaxial surface of the fourth and fifth leaves on the plant. After evaporation of the solvent, the epidermis imprint was visualized under a Zeiss Axiophot microscope with a Spot digital camera (Diagnostic Instruments). Cell size of leaflet epidermis was determined using the Image Pro-Plus software (Media Cybernetics). Leaflet surface was determined by scanning the same leaves used for epidermis imprint and the resulting image was analyzed using the Image Pro-Plus software.

RNA Extraction, Reverse Transcription-PCR Analysis, and DNA Construct Preparation

Total RNA extraction from tomato fruit and semiquantitative reverse transcription (RT)-PCR analysis using *SlGalLDH* gene-specific primers (Supplemental Table S1) were performed as described in Lemaire-Chamley et al. (2005). To obtain an *SlGalLDH*-specific cDNA fragment, RT (SuperScript II Reverse transcriptase) was performed using 2 μg of total RNA (Invitrogen, life technologies). A 133 bp *SlGalLDH* DNA fragment located in the 3'-untranslated region of the cDNA (GenBank accession no. AB080690) was then amplified by PCR using Ex Taq DNA polymerase (TaKaRa Bio INC) and the gene-specific primers GLDF4 and GLDR4. The purified DNA fragment was cloned as an inverted repeat under the control of the 35S promoter using the Gateway cloning system as described by Karimi et al. (2002), first into the entry vector (pDONR 201), then into the destination vector [pK7GWIWG2(1)]. This construct was checked by sequencing and introduced into cherry tomato ('West Virginia 106') plants by *Agrobacterium tumefaciens* strain GV3101 according to Hamza and Chupeau (1993). The first generation plants (T0) were characterized and screened. Of the 12 lines studied, four lines named 2, 5, 8, and 38 were selected for further detailed analyses in the T1 generation. Control plants correspond to plants transformed with an empty vector following the same protocol.

Experimental Design for Transcriptome and Metabolome Analyses

Plant materials used for these studies were the leaflet of the fourth leaf and the outer pericarp of the orange fruit. One-centimeter-length young leaves were tagged at the plant apex to allow comparison of leaflets at the same age and position on the plant. For fruit studies, flowers were tagged at anthesis (fully opened flower) and fruit were further selected according to their color measured on the external surface of fruit using a chromameter. The Lab values corresponding to orange stage were, respectively, L45, a = approximately 20, b = approximately 30. Once harvested, the leaflets and the outer pericarp were combined in pools of 10 to 15 samples, frozen in N_2, and stored at −80°C.

For transcript expression profiling of P_{35S}:*SlgalldhRNAi* silenced lines versus control plants, microarray experiments were performed using two biological repeats for each tissue (four slides per experiment) and technical duplicates with the dyes reversed (dye swap) as described in Lemaire-Chamley et al. (2005).

Microarray Analysis

Hybridization and Data Acquisition

The TOM1 cDNA microarrays (Center for Gene Expression at the Boyce Thompson Institute; http://bti.cornell.edu/CGEP/CGEP.html) contain 13,400 printed elements corresponding to approximately 8,700 unigenes (Alba et al., 2004). The Cyscribe Post Labeling kit from Amersham (catalog no. RPN5660X, Amersham Biosciences) was used according to the manufacturer's recommendations, with 30 μg of total RNA per condition. The pooled cy3- and cy5-labeled cDNAs were then concentrated on Microcon YM-30 columns (Amicon Bioseparations, Millipore) and mixed with 90 μL of hybridization solution containing 1:1 (v:v) formamide (5× SSC, 0.25% SDS, 5× Denhardt's solution, and 1 μg mL^{-1} denatured salmon sperm DNA [Stratagene]). Slides were hybridized in an automatic hybridization station HS 4800 (Tecan) with a washing prerun in 1× SSC, 0.1% SDS, for 1 min. The probe solution was boiled for 1 min and then injected into the hybridization chamber. Slides were incubated at 42°C for 16 h, with medium agitation, and then washed sequentially at 30°C in 1× SSC, 0.1% SDS for 1 min, this step was repeated three times, in 0.1× SSC, 0.1% SDS for 1 min, three times, and finally in 0.1× SSC for 30 s. Slides were dried in the hybridization station for 3 min, with 2.7 bars of nitrogen gas. Microarray slides were scanned with a Genepix 4000 B fluorescence reader (Axon Instruments) using Genepix 4.0 image acquisition software with photomultiplier tube voltage adjusted to 500 V for Cy3 and 600 V for Cy5.

Bioinformatic Analysis

Spot flagging was done first by Genepix (missing spots) and then by visual inspection of the images to exclude the bad spots (saturation and heterogeneity). Raw data files were submitted to LIMMA v2.3.3 Bioconductor package (Smyth et al., 2005; http://bioinf.wehi.edu.au/limma/). Negatively flagged spots were excluded from further analysis by giving them a zero weight value. Data were then normalized by the print-tip lowess method without background subtraction followed by the scale method to adjust the data between the slides. The correlation between the replicated spots was calculated (*duplicateCorrelation* function) and the linear model was fitted with the *lmFit* function for each gene, using this correlation. Moderated *t* statistics and log odds of differential expression were computed (*eBayes* function) for the contrast of interest (P_{35S}:*SlgalldhRNAi* transgenic line versus wild type) and for each gene. The calculated *P* values for this contrast were adjusted for multiple testing with the false discovery rate method. All analyses were performed using the default parameter setting of LIMMA.

In Situ Hybridization

To use *SlGalLDH* as a probe, riboprobes were synthesized from plasmids containing a 506 bp fragment of *SlGalLDH* cDNA obtained from tomato by PCR using GLDF1 and GLDR1 primers (Supplemental Table S1). The sense and antisense digoxygenin-labeled riboprobes were generated by run off transcription using T7 and SP6 RNA polymerases according to the manufacturer's protocol (Roche Diagnostics). For in situ hybridization, tomato flower buds, fruits of 7 and 20 DPA, young leaves, and shoot and root tips were sampled and processed as described by Bereterbide et al. (2002).

Production of a Rabbit Polyclonal Antibody Anti-*Sl*GalLDH and IgG Purification

For polyclonal antibody preparation, two synthetic polypeptides corresponding to the *Sl*GalLDH protein were prepared by the Eurogentec Company. Their sequences that were deduced from the *SlGalLDH* tomato gene (accession no. AB080690) were: *H2N*-MSKEKGPPKNKPKYT+*C-CONH2* (amino acids 321–335) and *H2N*-AYNQARKELDPNRIL+*C-CONH2* (amino acids 559–573). The +C corresponds to a Cys residue needed for the coupling with the keyhole limpet hemocyanin protein carrier. The antibodies were produced by rabbit immunized with a mix of the two peptides. Total IgGs were purified on affinity column (AF-amino TOYOPEARL 650 M) by Eurogentec.

Enzyme Activity, SDS-PAGE, and Immunodetection of *Sl*GalLDH

Fresh young leaves (approximately 0.5 g) were homogenized with a mortar and pestle in 1 mL of 0.1 M Tris-HCl buffer (pH 7.5) that contained 0.3 M Suc, 1% (w/v) polyvinylpolypyrrolidone, 0.2% (w/v) BSA, 1 mM dithiothreitol, and 50 mM EDTA. *Sl*GalLDH activity was assayed spectrophotometrically at room temperature by measuring the increase in A_{550} accompanied by the reduction of cytochrome *c* as described by Óba et al. (1995). Protein was quantified using BSA as a standard. Protein samples (10 μg per lane) were separated on 15% SDS-PAGE and transferred to Immobilon-P membrane prior to immunological detection by western-blot analysis using the *Sl*GalLDH antibody at 1:300 dilution. Antigen-antibody complexes were detected with horseradish peroxidase-conjugated IgG diluted 1:10,000 (Chemicon) with the BM Chemiluminescence blotting substrate (POD) system from Roche Applied Science.

Ascorbic Acid Analysis

Ascorbate analyses were performed according to Leipner et al. (1997). Between 0.5 and 1 g of frozen samples were homogenized in 2.5 mL of cold 3% (w/v) metaphosphoric acid and 2.5 mM EDTA. The homogenate was then centrifuged at 10,000*g* for 10 min at 4°C. An aliquot of 200 μL was incubated for 15 min at room temperature with 100 μL of K_2HPO_4 (45%), and either 50 μL of distilled water to measure the reduced ascorbate, or 50 μL of homo-Cys (0.1%) to measure the total ascorbate. After the incubation, 500 μL of citrate-P buffer (2 M, pH 2.3) were added. The A_{524} was measured immediately after addition of 500 μL 2,6-dichloroindophenol (0.008% w/v).

For measurement of apoplastic ascorbate content, the intercellular washing fluid (IWF) was prepared using a method similar to that described by Turcsányi et al. (2000). Leaflets of the fourth leaf (about 1 g) were washed in distilled water and were twice vacuum infiltrated (−70 kPa) for 3 min with 50 mL of 10 mM citrate buffer (pH 3.0) containing 100 mM KCl to reach maximum infiltration of cellular air spaces. Leaflets were then carefully blotted dry, rolled, and inserted into a 5 mL tip placed over a preweighed centrifuge tube containing 50 μL of 5% (w/v) cold metaphosphoric acid. The IWF (about 100 μL g^{-1} FW) was subsequently collected by centrifugation at 1,200*g* for 10 min at 4°C and immediately used for ascorbate measurement. The time from the harvest of the leaf to the beginning of centrifugation was less than 10 min. Activity of Glc-6-P dehydrogenase (EC 1.1.1.49), an enzyme located in the cytoplasm and the chloroplast stroma, was absent in the IWF, indicating that IWF was not contaminated by intracellular sap. To measure de novo ascorbate biosynthesis in leaves, 10 to 20 g of leaflet were rapidly washed in distilled water, sliced in fine stripes, and incubated at 25°C under continuous light (200 μmol photons m^{-2} s^{-1}) in Murashige and Skoog medium buffered with 100 mM Tris-HCl (pH 8.0) in the presence of 25 mM gulono-1,4-lactone or galactono-1,4-lactone (approximately 200 mg tissue in 5 mL medium). In time course of the incubation, the tissues were wringed on paper and snap frozen in liquid N_2, and stored at −80°C prior to ascorbate assay.

Determination of Levels of Other Metabolites

Samples of leaflets and orange fruit pericarp prepared as described above were used for metabolite extraction as described by Nunes-Nesi et al. (2005). The level of all metabolites was quantified by gas chromatography-mass spectrometry exactly following the protocol described by Roessner et al. (2001), with the exception that the peak identification was optimized to tomato tissues (Roessner-Tunali et al., 2003).

Sequence data from this article can be found in the GenBank/EMBL data libraries under accession number AB080690.

Supplemental Data

The following materials are available in the online version of this article.

Supplemental Table S1. Sets of PCR primers used to amplify specific regions of genes of interest.

Supplemental Table S2. Central metabolism of fully expanded leaf and orange fruit of P_{35S}:*Slgalldh*^{RNAi} transgenic and control plants.

LITERATURE CITED

Agius F, Gonzalez-Lamonthe R, Caballero JL, Munoz-Blanco L, Botella MA, Valpuesta V (2003) Engineering increased vitamin C levels in plants by over-expression of a D-galacturonic acid reductase. Nat Biotechnol 21: 177–181

Alba R, Fei Z, Payton P, Liu Y, Moore SL, Debbie P, Cohn J, D'Ascenzo M, Gordon JS, Rose JK, et al (2004) ESTs, cDNA microarrays, and gene expression profiling: tools for dissecting plant physiology and development. Plant J 39: 697–714

Andrews PK, Fahy DA, Foyer CH (2004) Relationships between fruit exocarp antioxidants in the tomato (Lycopersicon esculentum) high pigment-1 mutant during development. Physiol Plant 120: 519–528

Balmer Y, Vensel WH, Tanaka CK, Hurkman WJ, Gelhaye E, Rouhier N, Jacquot JP, Manieri W, Schurmann P, Droux M, et al (2004) Thioredoxin links redox to the regulation of fundamental processes of plant mitochondria. Proc Natl Acad Sci USA 101: 2642–2647

Bartoli CG, Guiamet JJ, Kiddle G, Pastori GM, Di Cagno R, Theodoulou FL, Foyer CH (2005) Ascorbate content of wheat leaves is not determined by maximal L-galactono-1,4-lactone dehydrogenase (GalLDH) activity under drought stress. Plant Cell Environ 28: 1073–1081

Bartoli CG, Pastori GM, Foyer CH (2000) Ascorbate biosynthesis in mitochondria is linked to the electron transport chain between complexes III and IV. Plant Physiol 123: 335–343

Bartoli CG, Yu J, Gómez F, Fernández L, McIntosh L, Foyer CH (2006) Inter-relationships between light and respiration in the control of ascorbic acid synthesis and accumulation in *Arabidopsis thaliana* leaves. J Exp Bot 57: 1621–1631

Bereterbide A, Hernould M, Farbos I, Glimelius K, Mouras A (2002) Restoration of stamen development and production of functional pollen in an alloplasmic CMS tobacco line by ectopic expression of the Arabidopsis thaliana. Plant J 29: 607–615

Bouché N, Fromm H (2004) GABA in plants: just a metabolite? Trends Plant Sci 9: 110–115

Burns JJ (1960) Ascorbic acid. *In* DM Greenberg, ed, Metabolic Pathway, Ed 2. Academic Press, New York, pp 394–411

Carrari F, Nunes-Nesi A, Gibon Y, Lytovchenko A, Loureiro ME, Fernie AR (2003) Reduced expression of aconitase results in an enhanced rate of photosynthesis and marked shifts in carbon partitioning in illuminated leaves of wild species tomato. Plant Physiol 133: 1322–1335

Cheniclet C, Rong WY, Causse M, Frangne N, Bolling L, Carde JP, Renaudin JP (2005) Cell expansion and endoreduplication show a large genetic variability in pericarp and contribute strongly to tomato fruit growth. Plant Physiol 139: 1984–1994

Davey MW, Gilot C, Persiau G, Østergaard J, Han Y, Bauw GC, Van Montagu MC (1999) Ascorbate biosynthesis in Arabidopsis cell suspension culture. Plant Physiol 121: 535–544

DeBolt S, Cook DR, Ford CM (2006) L-Tartaric acid synthesis from vitamin C in higher plants. Proc Natl Acad Sci USA 103: 5608–5613

Dutilleul C, Garnier M, Noctor G, Mathieu C, Chétrit P, Foyer CH, de Paepe R (2003) Leaf mitochondria modulate whole cell redox homeostasis, set antioxidant capacity, and determine stress resistance through altered signaling and diurnal regulation. Plant Cell 15: 1212–1226

Fernie AR, Trethewey RN, Krotzky AJ, Willmitzer L (2004) Metabolite profiling: from diagnostics to systems biology. Nat Rev Mol Cell Biol 5: 763–769

Ferrario S, Shchennikova AV, Franken J, Immink RG, Angenent GC (2006) Control of floral meristem determinacy in petunia by MADS-box transcription factors. Plant Physiol 140: 890–898

Geelen DNV, Inzé DG (2001) A bright future for the bright yellow-2 cell culture. Plant Physiol 127: 1375–1379

Giannino D, Condello E, Bruno L, Testone G, Tartarini A, Cozza R, Innocenti AM, Bitonti MB, Mariotti D (2004) The gene geranylgeranyl reductase of peach (Prunus persica [L.] Batsch) is regulated during leaf development and responds differentially to distinct stress factors. J Exp Bot 55: 2063–2073

Green MA, Fry SC (2005) Vitamin C degradation in plant cells via enzymatic hydrolysis of 4-O-oxalyl-L-threonate. Nature 344: 83–87

Hamza S, Chupeau Y (1993) Re-evaluation of conditions for plant regeneration and agrobacterium mediated transformation from tomato (Solanum esculantum). J Exp Bot 44: 1837–1845

Holtzapffel RC, Finnegan PM, Millar AH, Badger MR, Day DA (2002) Mitochondrial protein expression in tomato fruit during on-vine ripening and cold storage. Funct Plant Biol 29: 827–834

Horemans N, Potters G, De Wilde L, Caubergs RJ (2003) Division of tobacco bright yellow-2 cell cultures. Plant Physiol 133: 361–367

Jain AK, Nessler CL (2000) Metabolic engineering of an alternative pathway for ascorbic acid biosynthesis in plants. Mol Breed 6: 73–78

Karimi M, Inzé D, Depicker A (2002) Gateway vectors for Agrobacterium-mediated plant transformation. Trends Plant Sci 7: 193–195

Laing WA, Wright MA, Cooney J, Bulley SM (2007) The missing step of the L-galactose pathway of ascorbate biosynthesis in plants, an L-galactose guanyltransferase, increases leaf ascorbate content. Proc Natl Acad Sci USA 104: 9534–9539

Lancien M, Roberts MR (2006) Regulation of Arabidopsis thaliana 14-3-3 gene expression by gamma-aminobutyric acid. Plant Cell Environ 29: 1430–1436

Leipner J, Francheboub Y, Stamp P (1997) Accumulation by sub optimal growth temperature diminishes photooxidative damage in maize leaves. Plant Cell Environ 20: 366–372

Lemaire-Chamley M, Petit J, Garcia V, Just D, Baldet P, Germain V, Fagard M, Mouassite M, Cheniclet C, Rothan C (2005) Changes in transcriptional profiles are associated with early fruit tissue specialization in tomato. Plant Physiol 139: 750–769

Linster CL, Gomez TA, Christensen KC, Adler LN, Young BD, Brenner C, Clarke SG (2007) Arabidopsis VTC2 encodes a GDP-L-galactose phosphorylase, the last unknown enzyme in the Smirnoff-Wheeler pathway to ascorbic acid in plants. J Biol Chem 282: 18879–18885

Lorence A, Chevone B, Mendes P, Nessler C (2004) Myo-inositol oxygenase offers a possible entry point into plant ascorbate biosynthesis. Plant Physiol 134: 1200–1205

Millar AH, Mittova V, Kiddle G, Heazlewood JL, Bartoli CG, Theodoulou FL, Foyer CH (2003) Control of ascorbate synthesis by respiration and its implications for stress responses. Plant Physiol 133: 443–447

Mizukami Y (2001) A matter of size: developmental control of organ size in plants. Curr Opin Plant Biol 4: 533–539

Nelson DE, Rammesmayer G, Bohnert HJ (1998) Regulation of cell-specific inositol metabolism and transport in plant salinity tolerance. Plant Cell 10: 753–764

Noctor G, Foyer CH (1998) Ascorbate and glutathione: keeping active oxygen under control. Annu Rev Plant Physiol Plant Mol Biol 49: 249–279

Nunes-Nesi A, Carrari F, Lytovchenko A, Smith A, Loureiro M, Ratcliffe R, Sweetlove L, Fernie AR (2005) Enhanced photosynthetic performance and growth as a consequence of decreasing mitochondrial malate dehydrogenase activity in transgenic tomato plants. Plant Physiol 137: 611–622

Ôba K, Ishikawa S, Nishikawa M, Mizuno H, Yamamoto T (1995) Purification and properties of L-galactono-1,4-lactone dehydrogenase, a key enzyme for ascorbic acid biosynthesis, from sweet potato roots. J Biol Chem 117: 120–124

Olmos E, Kiddle G, Pellny TK, Kumar S, Foyer CH (2006) Modulation of plant morphology, root architecture, and cell structure by low vitamin C in Arabidopsis thaliana. J Exp Bot 57: 1645–1655

Parre E, Ghars MA, Leprince AS, Thiery L, Lefebvre D, Bordenave M, Richard L, Mazars C, Abdelly C, Savouré A (2007) Calcium signaling via phospho-

lipase C is essential for proline accumulation upon ionic but not nonionic hyperosmotic stresses in Arabidopsis. Plant Physiol 144: 503–512

Pastori GM, Kiddle G, Antoniw J, Bernard S, Veljovic-Jovanovic S, Verrier PJ, Noctor G, Foyer CH (2003) Leaf vitamin C contents modulate plant defense transcripts and regulate genes that control development through hormone signalling. Plant Cell 15: 939–951

Pignocchi C, Foyer CH (2003) Apoplastic ascorbate metabolism and its role in the regulation of cell signalling. Curr Opin Plant Biol 6: 379–389

Pignocchi C, Kiddle G, Hernandez I, Foster SJ, Asenti A, Taybi T, Barnes J, Foyer CH (2006) Ascorbate-oxidase-dependent changes in the redox state of the apoplast modulate gene transcript accumulation leading to modified hormone signalling and orchestration of defense processes in tobacco. Plant Physiol 141: 223–235

Raghavendra AS, Padmasree K (2003) Beneficial interactions of mitochondrial metabolism with photosynthetic carbon assimilation. Trends Plant Sci 8: 546–553

Rayle DL, Cleland RE (1992) The acid growth theory of auxin-induced cell elongation is alive and well. Plant Physiol 99: 1271–1274

Rhoads DM, Subbaiah CC (2007) Mitochondrial retrograde regulation in plants. Mitochondrion 7: 177–194

Roessner U, Luedemann A, Brust D, Fiehn O, Linke T, Willmitzer L, Fernie AR (2001) Metabolic profiling allows comprehensive phenotyping of genetically or environmentally modified plant systems. Plant Cell 13: 11–29

Roessner-Tunali U, Hegemann B, Lytovchenko A, Carrari F, Bruedigam C, Granot D, Fernie AR (2003) Metabolic profiling of transgenic tomato plant overexpressing hexokinase reveals that the influence of hexose phosphorylation diminishes during fruit development. Plant Physiol 133: 84–99

Smirnoff N (1996) The function and metabolism of ascorbic acid in plants. Ann Bot (Lond) 78: 661–669

Smirnoff N (2000) Ascorbic acid: metabolism and functions of a multi-facetted molecule. Curr Opin Plant Biol 3: 229–235

Smyth GK, Michaud J, Scott HS (2005) Use of within-array replicate spots for assessing differential expression in microarray experiments. Bioinformatics 21: 2067–2075

Suzuki N, Rizhsky L, Liang H, Shuman J, Shulaev V, Mittler R (2005) Enhanced tolerance to environmental stress in transgenic plants expressing the transcriptional coactivator multiprotein bridging factor 1c. Plant Physiol 139: 1313–1322

Tabata K, Ôba K, Suzuki K, Esaka M (2001) Generation and properties of ascorbic acid-deficient transgenic tobacco cells expressing antisense RNA for L-galactono-1,4-lactone dehydrogenase. Plant J 27: 139–148

Tamaoki M, Mukai F, Asai N, Nakajima N, Kubo A, Aono M, Saji H (2003) Light-controlled expression of a gene encoding L-galactono-1,4-lactone dehydrogenase which affects ascorbate pool size in Arabidopsis thaliana. Plant Sci 164: 1111–1117

Thimm O, Blasing O, Gibon Y, Nagel A, Meyer S, Kruger P, Selbig J, Muller LA, Rhee SY, Stitt M (2004) MAPMAN: a user-driven tool to display genomics data sets onto diagrams of metabolic pathways and other biological processes. Plant J 37: 914–939

Tokunaga T, Miyahara K, Tabata K, Esaka M (2005) Generation and properties of ascorbic acid-overproducing transgenic tobacco cells expressing sense RNA for L-galactono-1,4-lactone dehydrogenase. Planta 220: 854–863

Turcsányi E, Lyons T, Plöchl M, Barnes J (2000) Does ascorbate in the mesophyll cell walls form the first line of defence against ozone? Testing the concept using broad bean (vicia faba L.). J Exp Bot 51: 901–910

Urbanczyk-Wochniak E, Usadel B, Thimm O, Nunes-Nesi A, Carrari F, Davy M, Bläsing O, Kowalczyk M, Weicht D, Polinceusz A, et al (2006) Conversion of MapMan to allow the analysis of transcript data from Solanaceous species: effects of genetic and environmental alterations in energy metabolism in the leaf. Plant Mol Biol 60: 773–792

Wheeler G, Jones M, Smirnoff N (1998) The biosynthetic pathway of vitamin C in higher plants. Nature 393: 365–369

Wolucka BA, Van Montagu M (2003) GDP-mannose-3′,5′-epimerase forms GDP-L-gulose, a putative intermediate for the de novo biosynthesis of vitamin C in plants. J Biol Chem 278: 47483–47490

Yabuta Y, Mieda T, Rapolu M, Nakamura A, Motoki T, Matura T, Yoshimura K, Ishikawa T, Shigeoka S (2007) Light regulation of ascorbate biosynthesis is dependent on the photosynthetic electron chain but independent of sugars in Arabidopsis. J Exp Bot 58: 2661–2671

Zegzouti H, Jones B, Frasse P, Marty C, Maitre B, Latché A, Pech JC, Bouzayen M (1999) Ethylene-regulated gene expression in tomato fruit: characterization of novel ethylene-responsive and ripening-related genes isolated by differential display. Plant J 18: 589–600